The 15th International Conference on Advanced Robotics
Tallinn University of Technology
Tallinn, Estonia, June 20-23, 2011

# Dynamic Object Manipulation using a Multi-Fingered Hand-Arm System: Enhancement of a Grasping Capability using Relative Attitude Constraints of Fingers

Akihiro Kawamura, Kenji Tahara, Ryo Kurazume and Tsutomu Hasegawa

*Abstract*— **In this paper, an enhancement of a dynamic object grasping and manipulation method, which has been proposed by us previously, is presented. This enhancement makes it possible to grasp more various shaped objects which could not have been grasped by our previous method. In our previous method, a force/torque equilibrium condition to satisfy stable object grasping has been realized by only using grasping forces normal to an object surfaces. It is because each fingertip is soft and hemispheric and then rolling constraints arise during movement, and these phenomena cannot be stopped while existing the rolling constraint forces. Therefore, satisfying the dynamic force/torque equilibrium condition depends not only on a configuration of the multi-fingered hand system, but also on the shape of the grasped object. In this paper, a class of satisfying the force/torque equilibrium condition is expanded by generating counter tangential forces to suspend the rolling motion of each fingertip. In order to generate the counter tangential force, a relative attitude constraint between each finger is introduced. Firstly, a rolling constraint between each fingertip and object surface is given. Then, a relative attitude constraint control signal to generate constantly-produced tangential forces is designed. Finally, it is demonstrated through numerical simulations that the proposed control method accomplishes to grasp arbitrary shaped polyhedral objects and regulate its position and attitude, simultaneously.**

## I. Introduction

Humans perform dexterous manipulation tasks using their arms and hands. This ability is one of the most fundamental and important skills for robots working around humans. Aiming at this target, many robotic systems and control strategies for grasping and manipulation of an object have been proposed [1–4]. Among them, several methods related to a multi-fingered hand-arm system has been proposed to accomplish a dexterous grasping and manipulation tasks like a human hand [5–7]. We also have proposed the dynamic object grasping and its attitude control method for an arbitrary polyhedral shaped object using a multi-fingered hand-arm system with soft hemispherical fingertips, so far [8], [9]. This method can realize stable grasping and a desired object attitude by using a sensory feedback methodology. However,

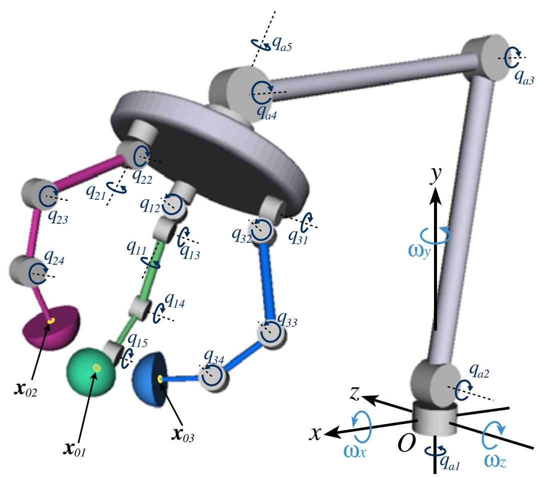


Fig. 1. Multi-fingered hand-arm system

several shaped objects are unable to grasp in stable using this method. In this method, a dynamic force/torque equilibrium condition to immobilize the object must be satisfied by only normal grasping forces component on each fingertip. It is because a tangential grasping force component induces a rolling motion of each fingertip. Namely, the tangential grasping force component on each fingertip must be vanished in order to satisfy a dynamic force/torque equilibrium condition in a final state. However, this requirement is quite strict, and hard to be satisfied in case of grasping an arbitrary polyhedral object. In order to relax the requirement, we add an another control signal which makes a counter tangential force to suspend a rolling motion of each fingertip and satisfy a desired force/torque equilibrium condition in a final state. Tahara *et al.* have proposed a stable object grasping and manipulation method that can generate a counter tangential force at the final state [10], [11]. However, this method cannot regulate a position and attitude of the grasped object to each desired value precisely. It is because their method uses a time integration of each joint angular velocity, and the integral term generates some deviations from a desired position and attitude of a grasped object. This paper proposes a novel object manipulation method to enhance our previously proposed one [8], [9]. A relative attitude constraint between each finger is introduced in addition to our previous controller. This artificial constraint makes a counter tangential force to cancel the tangential reaction force induced by the rolling motion of each fingertip. Using the artificial constraint forces makes it possible to grasp more various shaped objects. In addition, the dynamic stability of

This work was partially supported by "the Kyushu University Research Superstar Program (SSP)", based on the budget of Kyushu University allocated under President's initiative.

A. Kawamura is with the Graduate School of Information Science and Electrical Engineering, Kyushu University, Fukuoka, 819-0395, JAPAN kawamura@irvs.is.kyushu-u.ac.jp

K. Tahara is with the Faculty of Engineering, Kyushu University, Fukuoka, 819-0395, JAPAN tahara@ieee.org

R. Kurazume and T. Hasegawa are with the Faculty of Information Science and Electrical Engineering, Kyushu University, Fukuoka, 819-0395, JAPAN {kurazume, hasegawa}@ait.kyushu-u.ac.jp

978-1-4577-1157-2/11/$26.00 ©2011 IEEE

the overall system is ensured.

In what follows, firstly a nonholonomic rolling constraint between each fingertip and object surface is given. This rolling constraint is based on the Arimoto's model [10–13], and in this paper we expand Arimoto's model to the case that the object has an arbitrary polyhedral shape [8]. An arbitrary number of fingers are also allowed in our formulation. Secondly, Lagrange's equation of motion for the overall system is derived. After that, a control signal for stable grasping and manipulation of a grasped object with a new additional term to make a relative attitude constraint between each finger is designed. Finally, it is demonstrated through a numerical simulation that our control method makes it possible to grasp the arbitrary shaped polyhedral object with regulating a position and attitude of it. In addition, a detailed analysis of the stability for the closed-loop dynamics is shown in Appendix.

## II. A Multi Fingered Hand Arm System

In this section, a model of a hand-arm system is given. An example of the system treated here is illustrated in Fig. 1. This system has soft and hemispherical fingertips and enough number of DOFs to regulate a position and attitude of the grasped object. All fingertips maintain rolling contact with the object surfaces, and do not slip and detach from the surfaces during manipulation. It is assumed that each fingertip rolls within the ranges of its hemispheric surfaces, and they do not transfer to another surface during manipulation. Additionally, assume that object attitude information is available in real time by using some sort of external sensors (e.g. vision sensor, etc.). Note that the gravity effect is ignored in this paper in order to clarify a physical insight into analyzing physical interaction and stability of the system. As shown in Fig. 1, a symbol $O$ denotes the origin of Cartesian coordinates, and $\boldsymbol{x}_{0i} \in \mathbb{R}^3$ is the center position of each fingertip. Hereafter, a subscript $i$ refers to the $i^{\rm th}$ finger in all equations. The number of DOFs of the arm and the $i^{\rm f}$inger are $N_a$ and $N_i$, respectively. A joint angle vector of the arm is $\boldsymbol{q}_a \in \mathbb{R}^{N_a}$. Similarly, a joint angle vector of the $i^{\rm th}$ finger is $\boldsymbol{q}_{0i} \in \mathbb{R}^{\rm N_i}$. The joint angle vector of the overall system including the arm and all fingers is $\boldsymbol{q} = (\boldsymbol{q}_a, \boldsymbol{q}_{01}, \boldsymbol{q}_{02}, ..., \boldsymbol{q}_{0N})^{\rm T}$, where $N$ is the number of the fingers. As shown in Fig. 2, the center position of each contact area is $\boldsymbol{x}_i \in \mathbb{R}^3$, and a symbol $O_{c.m.}$ denotes the center position of an object mass and the origin of local coordinates. A position of $O_{c.m.}$ in Cartesian coordinates is $\boldsymbol{x} = (x, y, z)^{\rm T} \in \mathbb{R}^3$. An instantaneous rotational axis of the object at $O_{c.m.}$ in Cartesian coordinates is $\boldsymbol{\omega} = (\omega_x, \omega_y, \omega_z)^{\rm T} \in \mathbb{R}^3$.

### A. Constraints

A 3-dimensional rolling constraint with area contact is modeled here. Now, each contact frame at the center of each contact area is introduced. It is given as follows:

$$\boldsymbol{R}\cdot\boldsymbol{R}_{Ci} \quad = \quad (\boldsymbol{C}_{iX}, \boldsymbol{C}_{iY}, \boldsymbol{C}_{iZ}), \tag{1}$$

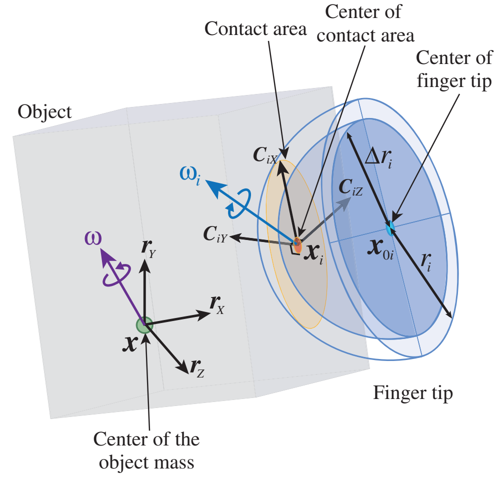


Fig. 2. Contact model at the center of each contact area

where $\boldsymbol{R}$ is a rotational matrix which expresses an attitude of the object in Cartesian coordinates, and $\boldsymbol{R}_{Ci}$ is a rotational matrix which expresses a relative attitude between the object frame to the contact frames. The $y$-axis of $\boldsymbol{R}_{Ci}$ is signified by a unit vector $\boldsymbol{C}_{iY}$ that is taken normal to the contact surface. Now, the rolling constraint can be expressed as Pfaffian constraints in the following form [8]:

$$\begin{bmatrix} \boldsymbol{X}_{iq} \\ \boldsymbol{Z}_{iq} \end{bmatrix} \dot{\boldsymbol{q}} + \begin{bmatrix} \boldsymbol{X}_{ix} \\ \boldsymbol{Z}_{ix} \end{bmatrix} \dot{\boldsymbol{x}} + \begin{bmatrix} \boldsymbol{X}_{i\omega} \\ \boldsymbol{Z}_{i\omega} \end{bmatrix} \boldsymbol{\omega} = \boldsymbol{0}, \tag{2}$$

where

$$\left[\begin{array}{l} \boldsymbol{X}_{iq} = \Delta r_i \boldsymbol{C}_{iZ}^{\rm T} \boldsymbol{J}_{\Omega i} - \boldsymbol{C}_{iX}^{\rm T} \boldsymbol{J}_{0i} \\ \boldsymbol{X}_{ix} = \boldsymbol{C}_{iX}^{\rm T} \\ \boldsymbol{X}_{i\omega} = \{\boldsymbol{C}_{iX} \times (\boldsymbol{x} - \boldsymbol{x}_{0i})\}^{\rm T} - \Delta r_i \boldsymbol{C}_{iZ}^{\rm T} \\ \boldsymbol{Z}_{iq} = -\Delta r_i \boldsymbol{C}_{iX}^{\rm T} \boldsymbol{J}_{\Omega i} - \boldsymbol{C}_{iZ}^{\rm T} \boldsymbol{J}_{0i} \\ \boldsymbol{Z}_{ix} = \boldsymbol{C}_{iZ}^{\rm T} \\ \boldsymbol{Z}_{i\omega} = \{\boldsymbol{C}_{iZ} \times (\boldsymbol{x} - \boldsymbol{x}_{0i})\}^{\rm T} + \Delta r_i \boldsymbol{C}_{iX}^{\rm T}, \end{array}\right. \tag{3}$$

and $\Delta r_i$ is the perpendicular distance between the center of each fingertip and contact surface (see Fig. 2). A symbol $\boldsymbol{J}_{\Omega_i} \in \mathbb{R}^{3\times\left(N_a+\sum_{i=1}^{N} N_i\right)}$ is the Jacobian matrix for the attitude angular velocity of each fingertip with respect to the joint angular velocity $\dot{\boldsymbol{q}} \in \mathbb{R}^{N_a+\sum_{i=1}^{N} N_i}$, and $\boldsymbol{J}_{0i} \in \mathbb{R}^{3\times\left(N_a+\sum_{i=1}^{N} N_i\right)}$ is the Jacobian matrix for the velocity of the center of each fingertip $\dot{\boldsymbol{x}}_{0i}$ with respect to the joint angular velocity, respectively.

### B. Contact Model of Soft Finger-Tip

The physical relationship between a deformation of the fingertip at the center of each contact area and its reproducing force is given on the basis of the lumped-parameterized model which have been proposed by Arimoto *et al* [12]. The reproducing force $f_i$ which is normal to the object surface at the center of each contact area is given as follows:

$$\left[\begin{array}{l} f_i = \bar{f}_i + \xi_i \frac{d}{dt}(r_i - \Delta r_i) \\ \bar{f}_i = k(r_i - \Delta r_i)^2, \end{array}\right. \tag{4}$$

where $r_i$ is the radius of each fingertip, $k$ is a positive stiffness constant and it depends on the material of the fingertip. Also, $\xi_i$ is a positive scalar function with respect to $\Delta r_i$, and it indicates that the viscous force depends on the contact area.

Additionally, we introduce another viscosity force between each fingertip and the object surfaces that affects toward a torsional motion around the normal vector $\boldsymbol{C}_{iY}$. The energy dissipation function to generate the torsional viscosity force is given as follows:

$$T_i = \frac{b_i}{2}||\boldsymbol{C}_{iY}^{\mathrm{T}}\left(\boldsymbol{\omega} - \boldsymbol{\omega}_i\right)||^2, \tag{5}$$

where $b_i$ is a positive scalar function which depends on the material of fingertip and the contact area, and $\boldsymbol{\omega}_i \in \mathbb{R}^3$ is an attitude angular velocity vector of each fingertip expressed by each contact frame.

### C. Overall Dynamics

Lagrange's equation of motion for the overall system considering the rolling constraint explicitly is given as follows: *For the multi-fingered hand-arm system:*

$$\boldsymbol{H}(\boldsymbol{q})\ddot{\boldsymbol{q}} + \left\{\frac{1}{2}\dot{\boldsymbol{H}}(\boldsymbol{q}) + \boldsymbol{S}(\boldsymbol{q}, \dot{\boldsymbol{q}})\right\}\dot{\boldsymbol{q}} + \sum_{i=1}^{N}\frac{\partial T_i}{\partial \dot{\boldsymbol{q}}}^{\mathrm{T}} + \sum_{i=1}^{N}\left(\boldsymbol{J}_{0i}^{\mathrm{T}}\boldsymbol{C}_{iY}f_i + \boldsymbol{X}_{iq}^{\mathrm{T}}\lambda_{iX} + \boldsymbol{Z}_{iq}^{\mathrm{T}}\lambda_{iZ}\right) = \boldsymbol{u}, \tag{6}$$

*For the object:*

$$\boldsymbol{M}\ddot{\boldsymbol{x}} + \sum_{i=1}^{N}\left(-f_i\boldsymbol{C}_{iY} + \boldsymbol{X}_{ix}^{\mathrm{T}}\lambda_{iX} + \boldsymbol{Z}_{ix}^{\mathrm{T}}\lambda_{iZ}\right) = \boldsymbol{0} \tag{7}$$

$$\boldsymbol{I}\dot{\boldsymbol{\omega}} + \boldsymbol{\omega}\times\boldsymbol{I}\boldsymbol{\omega} - \sum_{i=1}^{N}\{\boldsymbol{C}_{iY}\times(\boldsymbol{x} - \boldsymbol{x}_{0i})\}f_i + \sum_{i=1}^{N}\frac{\partial T_i}{\partial \boldsymbol{\omega}}^{\mathrm{T}} + \sum_{i=1}^{N}\left(\boldsymbol{X}_{i\omega}^{\mathrm{T}}\lambda_{iX} + \boldsymbol{Z}_{i\omega}^{\mathrm{T}}\lambda_{iZ}\right) = \boldsymbol{0}, \tag{8}$$

where $\boldsymbol{S}(\boldsymbol{q}, \dot{\boldsymbol{q}})$ signifies a skew-symmetric matrix, $\boldsymbol{u}$ stands for an input torque vector. In addition, $\lambda_{iX}$ and $\lambda_{iZ}$ denote Lagrange's multipliers.

## III. Control Input

In this section, a control signal for stable grasping and manipulation of an arbitrary polyhedral object is designed. The proposed controller consists of four parts, the first one is for stable grasping, the second one is for a position control, the third one is for an attitude control, and the last one is a newly added term to constrain a relative attitude between each finger to suspend the rolling motion of each fingertip. The first, second and third one are the same as previously proposed controller [8], [9]. The last one is the most different and remarkable point compared with the previous controller.

Firstly, a control signal for stable grasping $\boldsymbol{u}_s$ is designed so that the center of each fingertip approaches each other [8]. It is given as follows:

$$\boldsymbol{u}_s = \frac{f_d}{\sum_{i=1}^{N} r_i}\sum_{j=1}^{N}\boldsymbol{J}_{0j}^{\mathrm{T}}(\boldsymbol{x}_c - \boldsymbol{x}_{0j}) - \boldsymbol{C}\dot{\boldsymbol{q}}, \tag{9}$$

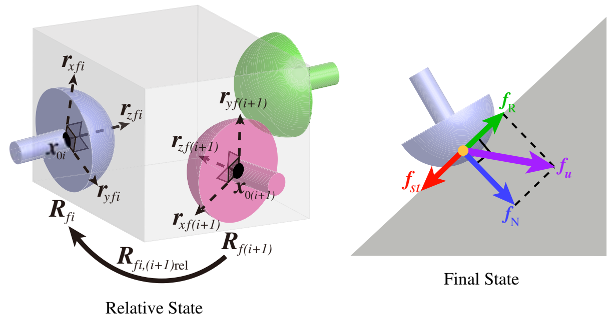


Fig. 3. Relative state and final state

where $\boldsymbol{C} \in \mathbb{R}^{\left(N_a + \sum_{i=1}^{N} N_i\right)\times\left(N_a + \sum_{i=1}^{N} N_i\right)} > 0$ is a positive definite diagonal matrix that expresses the damping gain for each joint. Also $f_d$ denotes a nominal desired grasping force, and $\boldsymbol{x}_c = \frac{1}{N}\sum_{i=1}^{N}\boldsymbol{x}_{0i}$.

Secondly, an object position control signal is designed. A position of the center of mass for the grasped object is commonly used as the object position. However, even using some external sensing methods, it is quite difficult to know an actual position of the center of mass during manipulation with no previous knowledge of the grasped object. In this study, we use $\boldsymbol{x}_c$ as a virtual object position instead of the actual position of the center of mass. The object position control signal $\boldsymbol{u}_p$ is given in the following:

$$\boldsymbol{u}_p = K_p\sum_{j=1}^{N}\boldsymbol{J}_{0j}^{\mathrm{T}}(\boldsymbol{x}_d - \boldsymbol{x}_c), \tag{10}$$

where $K_p$ is a positive scalar constant and $\boldsymbol{x}_d$ is a desired position of the object. In addition, we also introduce a control signal $\boldsymbol{u}_o$ to regulate an attitude of the grasped object. It is given as follows [9]:

$$\boldsymbol{u}_o = K_o\sum_{j=1}^{N}\boldsymbol{J}_{\Omega j}^{\mathrm{T}}\{(\boldsymbol{r}_x\times\boldsymbol{r}_{xd}) + (\boldsymbol{r}_y\times\boldsymbol{r}_{yd}) + (\boldsymbol{r}_z\times\boldsymbol{r}_{zd})\}, \tag{11}$$

where $K_o > 0$ is a positive scalar constant. A desired attitude of the object is expressed by a rotational matrix $\boldsymbol{R}_d = (\boldsymbol{r}_{xd}, \boldsymbol{r}_{yd}, \boldsymbol{r}_{zd})$. Also $\boldsymbol{r}_x\times\boldsymbol{r}_{xd}$ is an object attitude error vector with respect to the $x$-axis between a present attitude $\boldsymbol{r}_x$ and the desired attitude $\boldsymbol{r}_{xd}$. The attitude error vector with respect to other axes $y$ and $z$ can be defined in the similar way, and they are mutually orthonormal.Namely, the summation of these attitude error vectors indicates a desired instantaneous rotational axis of the object, and the desired object attitude can be realized if a contact force and moment from each finger is added to the object according to this desired axis.

Finally, a new control signal $\boldsymbol{u}_{st}$ to constrain a relative attitude of each finger is designed. This control signal generates a relative attitude constraint force between each finger. This artificial constraint force plays a role of a counter tangential force to cancel the rolling constraint force generated by the rolling motion (the rolling constraint force is expressed by

TABLE I

PHYSICAL PARAMETERS

Triple-fingered hand-arm system

| | | | | |
|---|---|---|---|---|
| $1^{\text{st}}$ link length | $l_{a1}$ | 1.300[m] | $l_{i1}$ | 0.300[m] |
| $2^{\text{nd}}$ link length | $l_{a2}$ | 1.000[m] | $l_{i2}$ | 0.200[m] |
| $3^{\text{rd}}$ link length | $l_{a3}$ | 0.175[m] | $l_{i3}$ | 0.140[m] |
| $1^{\text{st}}$ mass center | $l_{ga1}$ | 0.650[m] | $l_{gi1}$ | 0.150[m] |
| $2^{\text{nd}}$ mass center | $l_{ga2}$ | 0.500[m] | $l_{gi2}$ | 0.100[m] |
| $3^{\text{rd}}$ mass center | $l_{ga3}$ | 0.0875[m] | $l_{gi3}$ | 0.070[m] |
| $1^{\text{st}}$ mass | $m_{a1}$ | 1.300[kg] | $m_{i1}$ | 0.250[kg] |
| $2^{\text{nd}}$ mass | $m_{a2}$ | 1.000[kg] | $m_{i2}$ | 0.150[kg] |
| $3^{\text{rd}}$ mass | $m_{a3}$ | 0.400[kg] | $m_{i3}$ | 0.100[kg] |
| $1^{\text{st}}$ Inertia $\boldsymbol{I}_{a1}$ | $\mathrm{diag}(7.453, 7.453, 0.260)\times10^{-1}$[kg·m$^2$] | | | |
| $2^{\text{nd}}$ Inertia $\boldsymbol{I}_{a2}$ | $\mathrm{diag}(3.397, 3.397, 0.128)\times10^{-1}$[kg·m$^2$] | | | |
| $3^{\text{rd}}$ Inertia $\boldsymbol{I}_{a3}$ | $\mathrm{diag}(0.291, 0.291, 0.500)\times10^{-1}$[kg·m$^2$] | | | |
| $1^{\text{st}}$ Inertia $\boldsymbol{I}_{i1}$ | $\mathrm{diag}(7.725, 7.725, 0.450)\times10^{-3}$[kg·m$^2$] | | | |
| $2^{\text{nd}}$ Inertia $\boldsymbol{I}_{i2}$ | $\mathrm{diag}(2.060, 2.060, 0.120)\times10^{-3}$[kg·m$^2$] | | | |
| $3^{\text{rd}}$ Inertia $\boldsymbol{I}_{i3}$ | $\mathrm{diag}(0.538, 0.538, 0.031)\times10^{-3}$[kg·m$^2$] | | | |
| Radius of fingertip $r_i$ | 0.070[m] | | | |
| Stiffness coefficient $k_i$ | $1.000\times10^5$[N/m$^2$] | | | |
| Damping function $\xi_i$ | $1.000\times\left(r_i^2-\Delta r_i^2\right)\pi$[Ns/m$^2$] | | | |

Object

| | |
|---|---|
| Mass $m$ | 0.061[kg] |
| Length of each side | 0.42[m] |
| Inertia $\boldsymbol{I}$ | $\mathrm{diag}\,(4.589, 2.592, 4.589)\times10^{-2}$[kg · m$^2$] |

TABLE II

DESIRED GRASPING FORCE AND GAINS

| | |
|---|---|
| $f_d$ | 10.0[N] |
| $K_p$ | 3.333 |
| $K_o$ | 0.119 |
| $K_{st}$ | 4.286 |
| $\boldsymbol{C}_a$ | $\mathrm{diag}(1.003, 0.651, 0.735, 0.278, 0.177)\times10^{-1}$[Ns·m/rad] |
| $\boldsymbol{C}_1$ | $\mathrm{diag}(0.606, 0.687, 0.786, 0.642, 0.198)\times10^{-2}$[Ns·m/rad] |
| $\boldsymbol{C}_2$ | $\mathrm{diag}(0.468, 0.780, 0.318, 0.099)\times10^{-2}$[Ns·m/rad] |
| $\boldsymbol{C}_3$ | $\mathrm{diag}(0.648, 0.780, 0.318, 0.099)\times10^{-2}$[Ns·m/rad] |
| $\boldsymbol{x}_d$ | $(0.000, 0.450, 0.900)^{\mathrm{T}}$ [m] |
| $\boldsymbol{R}_d$ | $\begin{bmatrix} 0.82 & 0.21 & -0.54 \\ -0.22 & 0.97 & 0.05 \\ 0.53 & 0.08 & 0.84 \end{bmatrix}$ |

TABLE III

INITIAL CONDITION

| | |
|---|---|
| $\dot{\boldsymbol{q}}$ | $\boldsymbol{0}$[rad/s] |
| $\boldsymbol{q}_a$ | $(-0.176, -1.700, 1.903, 1.360, 0.519)^{\mathrm{T}}$ [rad] |
| $\boldsymbol{q}_{01}$ | $(0.014, 0.042, -0.997, 1.590, 0.306)^{\mathrm{T}}$ [rad] |
| $\boldsymbol{q}_{02}$ | $(0.011, -0.921, 1.218, 1.010)^{\mathrm{T}}$ [rad] |
| $\boldsymbol{q}_{03}$ | $(-0.056, -0.806, 1.074, 1.075)^{\mathrm{T}}$ [rad] |
| $\dot{\boldsymbol{x}}$ | $\boldsymbol{0}$ [m/s] |
| $\boldsymbol{x}$ | $(-0.120, 0.529, 0.775)^{\mathrm{T}}$ [m] |
| $\boldsymbol{\omega}$ | $\boldsymbol{0}$ [rad/s] |
| $\boldsymbol{R}$ | $\begin{bmatrix} 0.77 & 0.07 & -0.67 \\ -0.04 & 1.00 & 0.05 \\ 0.67 & -0.01 & 0.74 \end{bmatrix}$ |

$\boldsymbol{f}_{\mathrm{R}}$ in Fig. 3). Namely, the dynamic force/torque equilibrium condition to immobilize a grasped object can be realized by the artificial tangential constraint force $\boldsymbol{f}_{st}$ because the rolling motion of each finger can be suspended by this artificial constraint forces. The control signal for the relative attitude constraint between each finger $\boldsymbol{u}_{st}$ is given as follows:

$$\begin{aligned} \boldsymbol{u}_{st} \;=\; K_{st}\sum_{i=1}^{N}\boldsymbol{J}_{\Omega i}^{\mathrm{T}}\Big\{&\boldsymbol{r}_{xfi}\times\left(\boldsymbol{r}_{xfi,(i-1)d}+\boldsymbol{r}_{xfi,(i+1)d}\right)\\ &+\boldsymbol{r}_{yfi}\times\left(\boldsymbol{r}_{yfi,(i-1)d}+\boldsymbol{r}_{yfi,(i+1)d}\right)\\ &+\boldsymbol{r}_{zfi}\times\left(\boldsymbol{r}_{zfi,(i-1)d}+\boldsymbol{r}_{zfi,(i+1)d}\right)\Big\}, \end{aligned} \tag{12}$$

where

$$\boldsymbol{R}_{fi} = \left(\boldsymbol{r}_{xfi}, \boldsymbol{r}_{yfi}, \boldsymbol{r}_{zfi}\right) \tag{13}$$

$$\begin{aligned} \boldsymbol{R}_{fi,jd} &= \left(\boldsymbol{r}_{xfi,jd}, \boldsymbol{r}_{yfi,jd}, \boldsymbol{r}_{zfi,jd}\right)\\ &= \boldsymbol{R}_{fj}\boldsymbol{R}_{fi,j\mathrm{rel}}, \quad \left(j=(i-1),(i+1)\right) \end{aligned} \tag{14}$$

where $K_{st}>0$ is a positive scalar constant. Both $\boldsymbol{R}_{fi}$ and $\boldsymbol{R}_{fi,jd}$ are rotational matrices that express a present and desired attitude of $i^{\text{th}}$ fingertip, respectively. Also $\boldsymbol{R}_{fi,j\mathrm{rel}}$ is a relative rotational matrix between an attitude of $i^{\text{th}}$ and $j^{\text{th}}$ fingers. In Fig. 3, $\boldsymbol{f}_{\boldsymbol{u}}$ is a grasping force generated by the control signal of stable grasping and manipulation of the object except that generated by the relative attitude constraint input $\boldsymbol{u}_{st}$. Therefore, the total control signal $\boldsymbol{u}$ is given as follows:

$$\boldsymbol{u} = \boldsymbol{u}_s + \boldsymbol{u}_p + \boldsymbol{u}_o + \boldsymbol{u}_{st}. \tag{15}$$

The stability of the overall system can be verified. It can be found in Appendix.

## IV. NUMERICAL SIMULATION

Numerical simulations to show the effectiveness of proposed controller is conducted here. In the simulations, a desired relative attitude constraint $\boldsymbol{R}_{fi,j\mathrm{rel}}$ in (14) is configured to keep an initial relative attitude of all fingertips. It is given in the following:

$$\boldsymbol{R}_{fi,j\mathrm{rel}} = \boldsymbol{R}_{fj\mathrm{ini}}^{\mathrm{T}}\boldsymbol{R}_{fi\mathrm{ini}}, \tag{16}$$

where $\boldsymbol{R}_{fi\mathrm{ini}}$ is a rotational matrix between an initial attitude of $i^{\text{th}}$ fingers. A hand-arm system used in the simulation is that it consists of an arm part which has 5 DOFs and a triple-fingered hand part which has one 5 DOFs finger and two 4 DOFs fingers. The shape of the grasped object is a hexahedron that is made of combining two tetrahedrons, and it cannot satisfy the force/torque equilibrium condition by only using normal grasping force components. Namely, this grasped object cannot be grasped by only using our previous controller [8], [9]. The parameters of the triple-fingered hand-arm system and the object are shown in Table I. Table II shows a desired nominal grasping force, each gain and a desired position and attitude of the grasped object. Table III shows an initial condition. Figures 4 and 5 show the transient responses of the object position and attitude. We see from these figures that both the position and attitude of the object converge to each desired value, respectively. Additionally, we also confirmed that the elements of $\boldsymbol{\Delta\lambda}_{\infty}$ and the velocities of the overall system converge to zero. These results indicate that our proposed controller realizes stable grasping and the desired position and attitude of the object, even it cannot satisfy the force/torque equilibrium condition by only using normal grasping forces. In addition to the simulation, we conduct another simulation without the new control signal $\boldsymbol{u}_{st}$. The top figure in Fig. 6 shows an initial state of the simulation, and the lower two figures show the state at 5 seconds later. We can see the effectiveness of $\boldsymbol{u}_{st}$ to suspend the rolling motion of the fingertips through Fig. 6.

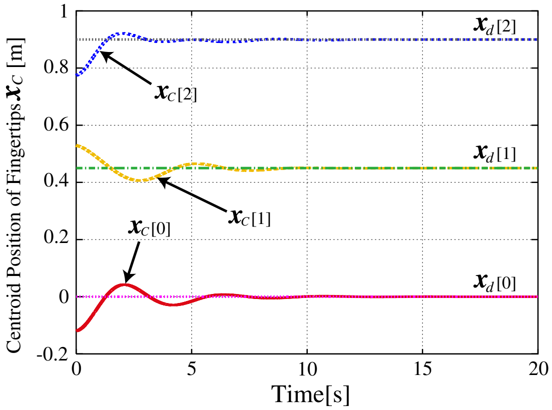


Fig. 4. Transient responses of the centroid position of fingertips $\boldsymbol{x}_C$

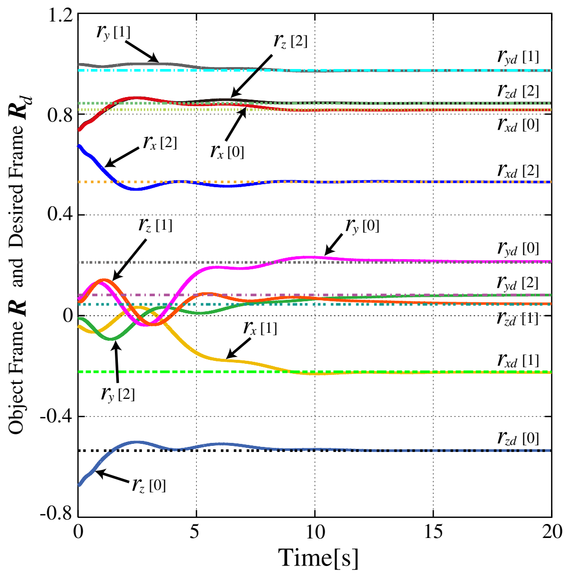


Fig. 5. Transient responses of the object frame $\boldsymbol{R} = (\boldsymbol{r}_x, \boldsymbol{r}_y, \boldsymbol{r}_z)$

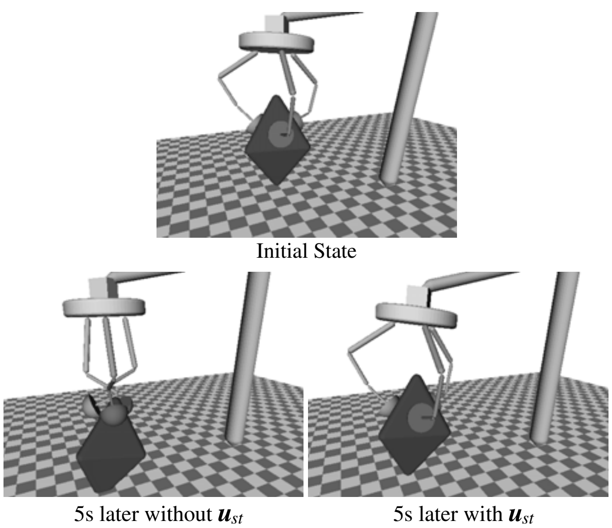


Fig. 6. Simulation for a position and attitude control of the grasped object

## V. Conclusion

This paper presented the new control signal to enhance the dynamic object grasping and manipulation method we have proposed previously in order to be able to grasp a more various shaped object using the relative attitude constraint between fingers. Firstly, we formulated the nonholonomic rolling constraint. Next, the new control signal to constrain the relative attitude between fingers was designed in addition to our previously proposed grasping and manipulation controller. After that, it was verified through the numerical simulations that the proposed method realized the desired position and attitude of the object stably, even in the case that the force/torque equilibrium condition cannot be satisfied by only using the normal grasping force component. In addition, the stability of the overall system was verified by analyzing the closed-loop dynamics in Appendix. In our future works, we will conduct some experiments to verify a practical usefulness of our proposed method. Furthermore, we will expand the proposed control scheme for an object with arbitrary smooth curved surfaces.

## Acknowledgment

This work was partially supported by "the Kyushu University Research Superstar Program (SSP)", based on the budget of Kyushu University allocated under President's initiative and Grant-in-Aid for JSPS Fellows.

## References

[1] M. R. Cutkosky, *Grasping and Fine Manipulation*, Kluwer Academic, Dordrecht, Netherlands; 1985.

[2] R. M. Murray, Z. Li and S. S. Sastry, *Mathematical Introduction to Robotic Manipulation*, CRC Press, Boca Raton; 1994.

[3] A. M. Okamura, N. Smaby and M. R. Cutkosky, "An overview of dexterous manipulation," *Proc. of the 2000 IEEE Int. Conf. Robot. Automat.*, pp. 255–262, SanFrancisco, CA, 2000.

[4] A. Bicchi, "Hands for dexterous manipulation and robust grasping: A difficult road towards simplicity," *IEEE Trans. Robot. Automat.*, vol. 16, no. 6, pp. 652–662, 2000.

[5] K. Ohnishi, T. Tajima and Y. Saito, "Anthropomorphic hand control for robotic hand-arm system," *IEEE Transactions on Systems, Man, and Cybernetics,* , vol.2, pp. 1255–1259, Nashville, TN, 2000.

[6] K. Nagai and T. Yoshikawa, "Grasping and manipulation by arm/multifingered-hand mechanisms," *Proc. of the 1995 IEEE Int. Conf. on Robotics and Automation*, pp. 1040–1047, May 21-27, Nagoya, Japan, 1995.

[7] J.-H. Bae, S. Arimoto, R. Ozawa, M. Sekimoto and M. Yoshida, "A unified control scheme for a whole robotic arm-fingers system in grasping and manipulation," *Proc. of the 2006 IEEE Int. Conf. Robot. Automat.*, pp. 2131–2136, Orlando, Florida, 2006.

[8] A. Kawamura, K. Tahara, R. Kurazume and T. Hasegawa, "Dynamic Grasping for an Arbitrary Polyhedral Object by a Multi-fingered Hand-Arm System," *2009 IEEE/RSJ Int. Conf. on Intelligent Robots and Systems*, pp. 2264–2270, St. Louis, Missouri, 2009.

[9] A. Kawamura, K. Tahara, R. Kurazume and T. Hasegawa, "Dexterous Object Manipulation by a Human-Like Hand-Arm System with Unified Controller," *1st Int. Conf. on Applied Bionics and Biomechanics*, Venice, Italy, 2010 (to appear).

[10] K. Tahara, S. Arimoto and M. Yoshida, "Dynamic force/torque equilibrium for stable grasping by a triple robotic fingers system," *Proc. IEEE/RSJ Int. Conf. Intell. Robots, Syst.*, pp. 2257–2263, St. Louis, MO, 2009.

[11] K. Tahara, S. Arimoto and M. Yoshida, "Dynamic object manipulation using a virtual frame by a triple soft-fingered robotic hand," *Proc. of the 2010 IEEE Int. Conf. Robot. Automat.*, pp. 4322–4327, Anchorage, AK, 2010.

[12] S. Arimoto, P.T.A. Nguyen, H.-Y. Han and Z. Doulgeri, "Dynamics and control of a set of dual fingers with soft tips," *Robotica*, vol. 18, no. 1, pp. 71–80, 2000.

[13] S. Arimoto, "A differential-geometric approach for 2-D and 3-D object grasping and manipulation," *Annual Review in Control*, Vol. 31, pp. 189–209, 2007.

## Appendix

The stability of the system is proved here. The closed-loop dynamics of the overall system is given by substituting (15) into (6) such that

*For the multi-fingered hand-arm system:*

$$\begin{aligned}&\boldsymbol{H}\ddot{\boldsymbol{q}} + \left\{\frac{1}{2}\dot{\boldsymbol{H}} + \boldsymbol{S} + \boldsymbol{C}\right\}\dot{\boldsymbol{q}} + \sum_{i=1}^{N} \boldsymbol{J}_{0i}^{\mathrm{T}} \boldsymbol{C}_{iY} \Delta f_i \\ &\quad + \sum_{i=1}^{N} \boldsymbol{X}_{iq}^{\mathrm{T}} \Delta\lambda_{iX} + \sum_{i=1}^{N} \boldsymbol{Z}_{iq}^{\mathrm{T}} \Delta\lambda_{iZ} + \sum_{i=1}^{N} \frac{\partial T_i}{\partial \dot{\boldsymbol{q}}}^{\mathrm{T}} \\ &\quad + \sum_{i=1}^{N} \boldsymbol{J}_{\Omega i}^{\mathrm{T}} (\boldsymbol{x}_i - \boldsymbol{x}_{0i}) \times \boldsymbol{x}_{tr} + \sum_{i=1}^{N} \boldsymbol{C}_{iY}^{\mathrm{T}} \boldsymbol{B} \boldsymbol{J}_{\Omega i}^{\mathrm{T}} \boldsymbol{C}_{iY} \\ &\quad + \sum_{i=1}^{N} \left\{-\frac{1}{\Delta r_i} \boldsymbol{J}_{0i}^{\mathrm{T}} (\boldsymbol{B} \times \boldsymbol{C}_{iY})\right\} = \boldsymbol{0}, \end{aligned} \tag{17}$$

*For the object:*

$$\begin{aligned}&\boldsymbol{M}\ddot{\boldsymbol{x}} + \sum_{i=1}^{N} \left(-\Delta f_i \boldsymbol{C}_{iY} + \boldsymbol{X}_{ix}^{\mathrm{T}} \Delta\lambda_{iX} + \boldsymbol{Z}_{ix}^{\mathrm{T}} \Delta\lambda_{iZ}\right) \\ &\quad - \sum_{i=1}^{N} \left\{\boldsymbol{x}_{tr} - \frac{1}{\Delta r_i} (\boldsymbol{B} \times \boldsymbol{C}_{iY})\right\} = \boldsymbol{0} \end{aligned} \tag{18}$$

$$\begin{aligned}&\boldsymbol{I}\dot{\boldsymbol{\omega}} + \boldsymbol{\omega} \times \boldsymbol{I}\boldsymbol{\omega} - \sum_{i=1}^{N} \{\boldsymbol{C}_{iY} \times (\boldsymbol{x} - \boldsymbol{x}_{0i})\} \Delta f_i \\ &\quad + \sum_{i=1}^{N} \left(\boldsymbol{X}_{i\omega}^{\mathrm{T}} \Delta\lambda_{iX} + \boldsymbol{Z}_{i\omega}^{\mathrm{T}} \Delta\lambda_{iZ}\right) + \sum_{i=1}^{N} \frac{\partial T_i}{\partial \boldsymbol{\omega}}^{\mathrm{T}} \\ &\quad + \sum_{i=1}^{N} (\boldsymbol{x} - \boldsymbol{x}_i) \times \left(\boldsymbol{x}_{tr} - \frac{1}{\Delta r_i} \boldsymbol{B} \times \boldsymbol{C}_{iY}\right) = \boldsymbol{0}, \end{aligned} \tag{19}$$

where

$$\left[\begin{array}{l} A = \frac{f_d}{\sum_{j=1}^{N} \Delta r_j} \\ \boldsymbol{x}_{tr} = A(\boldsymbol{x}_c - \boldsymbol{x}_{0i}) + K_p(\boldsymbol{x}_d - \boldsymbol{x}_c) \\ \boldsymbol{B} = K_{st}\boldsymbol{B}_{st} + K_o\boldsymbol{B}_o \\ \boldsymbol{B}_{st} = (\boldsymbol{r}_{xfj} \times \boldsymbol{r}_{xfjd}) + (\boldsymbol{r}_{yfj} \times \boldsymbol{r}_{yfjd}) \\ \qquad\qquad + (\boldsymbol{r}_{zfj} \times \boldsymbol{r}_{zfjd}) \\ \boldsymbol{B}_o = (\boldsymbol{r}_{xd} \times \boldsymbol{r}_x) + (\boldsymbol{r}_{yd} \times \boldsymbol{r}_y) + (\boldsymbol{r}_{zd} \times \boldsymbol{r}_z) \\ \Delta f_i = f_i - \boldsymbol{C}_{iY}^{\mathrm{T}} \boldsymbol{x}_{tr} \\ \Delta\lambda_{iX} = \lambda_{iX} + \boldsymbol{C}_{iX}^{\mathrm{T}} \boldsymbol{x}_{tr} + \frac{1}{\Delta r_i} \boldsymbol{C}_{iZ}^{\mathrm{T}} \boldsymbol{B} \\ \Delta\lambda_{iX} = \lambda_{iZ} + \boldsymbol{C}_{iZ}^{\mathrm{T}} \boldsymbol{x}_{tr} - \frac{1}{\Delta r_i} \boldsymbol{C}_{iX}^{\mathrm{T}} \boldsymbol{B} \end{array}\right. \tag{20}$$

Now, an output vector of the overall system is given as follows:

$$\dot{\boldsymbol{\Lambda}} = \left(\dot{\boldsymbol{q}}^{\mathrm{T}}, \dot{\boldsymbol{x}}^{\mathrm{T}}, \boldsymbol{\omega}^{\mathrm{T}}\right)^{\mathrm{T}}. \tag{21}$$

By taking a sum of the inner product of (21) and the closed loop dynamics expressed by (17), (18) and (19), we obtain

$$\frac{d}{dt}E = -\dot{\boldsymbol{q}}^{\mathrm{T}} \boldsymbol{C} \dot{\boldsymbol{q}} - \sum_{i=1}^{N} \left(T_i + \xi \Delta \dot{r}_i^2\right) - D \leq 0 \tag{22}$$

$$E = K + V + \Delta P \geq 0 \tag{23}$$

$$K = \frac{1}{2} \dot{\boldsymbol{q}}^{\mathrm{T}} \boldsymbol{H} \dot{\boldsymbol{q}} + \frac{1}{2} \dot{\boldsymbol{x}}^{\mathrm{T}} \boldsymbol{M} \dot{\boldsymbol{x}} + \frac{1}{2} \boldsymbol{\omega}^{\mathrm{T}} \boldsymbol{I} \boldsymbol{\omega} \tag{24}$$

$$V = V_s + V_p + V_o \tag{25}$$

$$V_s = \frac{A}{4N} \left\{\sum_{i=1}^{N} \sum_{j=1}^{N} (\boldsymbol{x}_{0i} - \boldsymbol{x}_{0j})^2\right\} \tag{26}$$

$$V_p = \frac{N K_p}{2} (\boldsymbol{x}_d - \boldsymbol{x}_c)^2 \tag{27}$$

$$\begin{aligned}V_o = \frac{N K_o}{2} &\left\{(\boldsymbol{r}_x - \boldsymbol{r}_{xd})^2 + (\boldsymbol{r}_y - \boldsymbol{r}_{yd})^2\right. \\ &\left. + (\boldsymbol{r}_z - \boldsymbol{r}_{zd})^2\right\}\end{aligned} \tag{28}$$

$$\Delta P = \sum_{i=1}^{N} \int_0^{\delta r_i} \left\{\bar{f}_i(\Delta r_{di} + \phi) - \bar{f}_i(\Delta r_{di})\right\} d\phi, \tag{29}$$

where

$$\delta r_i = \Delta r_{di} - \Delta r_i \tag{30}$$

$$D = D_{st} + D_o \tag{31}$$

$$\begin{aligned}D_{st} &= \frac{d}{dt}\left\{K_{st} \sum_{i=1}^{N} \mathrm{tr}\left(\boldsymbol{R}_{fi}^{\mathrm{T}} \boldsymbol{R}_{f(i+1)} \boldsymbol{R}_{fi,(i+1)\mathrm{rel}}\right)\right\} \\ &= \frac{d}{dt}\left\{K_{st} \sum_{i=1}^{N} (1 + 2\cos\alpha_i)\right\}\end{aligned} \tag{32}$$

$$D_o = \sum_{i=1}^{N} \frac{K_o}{\Delta r_i} \left[\frac{d}{dt} \{\boldsymbol{C}_{iY} \times (\boldsymbol{x} - \boldsymbol{x}_{0i})\}\right]^{\mathrm{T}} \boldsymbol{B}. \tag{33}$$

In (30), $\Delta r_{di}$ is $\Delta r_i$ when $f_i$ equals to $f_d$. In (32), $\alpha_i$ is a rotational angle of $\boldsymbol{R}_{fi}^{\mathrm{T}} \boldsymbol{R}_{f(i+1)} \boldsymbol{R}_{f(i+1)\mathrm{rel}}^{\mathrm{T}} \boldsymbol{R}_{fi\mathrm{rel}}$. The scalar function $V$ plays a role of an artificial potential energy arising from the control input. Also $K$, $V$ and $\Delta P$ are positive as long as $0 \leq \Delta r_{di} - \delta r_i < r_i$, thereby (23) is satisfied. Equation (33) can be rearranged as follows [9]:

$$D_o = \sum_{i=1}^{N} 2K_o \cos\beta \frac{d}{dt} \log \Delta r_i, \tag{34}$$

where $\beta$ is a rotational angle from an initial attitude to a desired attitude. From (22) and $|\cos\beta| \leq 1$, we obtain

$$\begin{aligned}&\frac{d}{dt}E + D_{st} - \left|\sum_{i=1}^{N} 2K_o \frac{d}{dt} \log \Delta r_i\right| \\ &\qquad \leq -\dot{\boldsymbol{q}}^{\mathrm{T}} \boldsymbol{C} \dot{\boldsymbol{q}} - \sum_{i=1}^{N} \left(T_i + \xi \Delta \dot{r}_i^2\right).\end{aligned} \tag{35}$$

Now, we define a new scalar function $a$ as follows:

$$\left\{\begin{array}{lll} a = 1 & \text{if} & \sum_{i=1}^{N} 2K_o \frac{d}{dt} \log \Delta r_i \geq 0 \\ a = -1 & & \text{otherwise.} \end{array}\right. \tag{36}$$

Then, (35) is rearranged using $a$ as follows:

$$\frac{d}{dt}W \leq -\dot{\boldsymbol{q}}^{\mathrm{T}} \boldsymbol{C} \dot{\boldsymbol{q}} - \sum_{i=1}^{N} \left(T_i + \xi \Delta \dot{r}_i^2\right) \leq 0, \tag{37}$$

where

$$W = E + K_{st}\sum_{i=1}^{N}(1+2\cos\alpha_i) - a\sum_{i=1}^{N}2K_o\log\Delta r_i. \quad (38)$$

Furthermore, we obtain

$$\begin{aligned} W &\geq E + K_{st}\sum_{i=1}^{N}(1+2\cos\alpha_i) - a\sum_{i=1}^{N}2K_o\log\Delta r_i \\ &\geq E - NK_{st} - \left|\sum_{i=1}^{N}2K_o\log\Delta r_i\right|. \end{aligned} \quad (39)$$

The following equation is obtained if the right-hand side of (39) is positive.

$$W \geq 0. \quad (40)$$

In other words, (40) is satisfied as long as all gains in the control input are designed to satisfy the following equation

$$E - NK_{st} - \left|\sum_{i=1}^{N}2K_o\log\Delta r_i\right| \geq 0. \quad (41)$$

Equations (37) and (40) yield

$$\begin{aligned} &\int_0^\infty \left\{\dot{\boldsymbol{q}}^{\mathrm{T}}\boldsymbol{C}\dot{\boldsymbol{q}} + \sum_{i=1}^{N}\left(T_i + \xi\Delta\dot{r}_i^2\right)\right\}dt \\ &\qquad \leq W(0) - W(\infty) \leq W(0). \end{aligned} \quad (42)$$

Equation (42) shows that the joint angular velocity $\dot{\boldsymbol{q}}(t)$ is squared integrable over time $t \in [0,\infty)$. It indicates $\dot{\boldsymbol{q}}(t) \in L^2(0,\infty)$. Considering the rolling constraint shown by (2), it is also clear that $\dot{\boldsymbol{x}} \in L^2(0,\infty)$ and $\boldsymbol{\omega} \in L^2(0,\infty)$. Thereby, the output of the overall system $\dot{\boldsymbol{\Lambda}}(t)$ is uniformly continuous and it is shown that $\dot{\boldsymbol{\Lambda}} \to \boldsymbol{0}$ and $\ddot{\boldsymbol{\Lambda}} \to \boldsymbol{0}$ as $t \to \infty$ [13]. Therefore, it is obvious that the sum of the nominal external forces affecting on the hand-arm system and the object $\boldsymbol{\Delta\lambda}_\infty$ converge to zero.

$$\boldsymbol{\Delta\lambda}_\infty = (\boldsymbol{\Delta\lambda_q}, \boldsymbol{\Delta\lambda_x}, \boldsymbol{\Delta\lambda_\omega}) \to \boldsymbol{0}, \quad (43)$$

where

$$\begin{aligned} \boldsymbol{\Delta\lambda_q} &= \sum_{i=1}^{N}\left(\boldsymbol{J}_{0i}^{\mathrm{T}}\boldsymbol{C}_{iY}\Delta f_i + \boldsymbol{X}_{iq}^{\mathrm{T}}\Delta\lambda_{iX} + \boldsymbol{Z}_{iq}^{\mathrm{T}}\Delta\lambda_{iZ}\right) \\ &+ \sum_{i=1}^{N}\boldsymbol{J}_{\Omega i}^{\mathrm{T}}(\boldsymbol{x}_i - \boldsymbol{x}_{0i}) \times \boldsymbol{x}_{tr} \\ &+ \sum_{i=1}^{N}\left\{K_o\boldsymbol{C}_{iY}^{\mathrm{T}}\boldsymbol{B}\boldsymbol{J}_{\Omega i}^{\mathrm{T}}\boldsymbol{C}_{iY} - \frac{1}{\Delta r_i}\boldsymbol{J}_{0i}^{\mathrm{T}}(\boldsymbol{B}\times\boldsymbol{C}_{iY})\right\} \end{aligned} \quad (44)$$

$$\begin{aligned} \boldsymbol{\Delta\lambda_x} &= \sum_{i=1}^{N}\left(-\Delta f_i\boldsymbol{C}_{iY} + \boldsymbol{X}_{ix}^{\mathrm{T}}\Delta\lambda_{iX} + \boldsymbol{Z}_{ix}^{\mathrm{T}}\Delta\lambda_{iZ}\right) \\ &- \sum_{i=1}^{N}\left\{\boldsymbol{x}_{tr} - \frac{1}{\Delta r_i}(\boldsymbol{B}\times\boldsymbol{C}_{iY})\right\} \end{aligned} \quad (45)$$

$$\begin{aligned} \boldsymbol{\Delta\lambda_\omega} &= -\sum_{i=1}^{N}\{\boldsymbol{C}_{iY}\times(\boldsymbol{x}-\boldsymbol{x}_{0i})\}\Delta f_i \\ &+ \sum_{i=1}^{N}\left(\boldsymbol{X}_{i\omega}^{\mathrm{T}}\Delta\lambda_{iX} + \boldsymbol{Z}_{i\omega}^{\mathrm{T}}\Delta\lambda_{iZ}\right) \\ &+ \sum_{i=1}^{N}(\boldsymbol{x}-\boldsymbol{x}_i)\times\left\{\boldsymbol{x}_{tr} - \frac{1}{\Delta r_i}(\boldsymbol{B}\times\boldsymbol{C}_{iY})\right\}, \end{aligned} \quad (46)$$

where $\boldsymbol{\Delta\lambda_q}$ denotes an external force applied to each joint of the hand-arm system. Also $\boldsymbol{\Delta\lambda_x}$ and $\boldsymbol{\Delta\lambda_\omega}$ are external forces affecting on the object.

As a consequence, it is shown that the desired position and attitude of the object is realized stably, because each nominal external force and velocity becomes zero.